Article

I-124 Labeled Anthraquinone-Derivative-Coating Gold Nanoparticles for Targeted Breast Cancer Diagnosis and Therapy

Jun Young Lee and Jeong Hoon Park *

Posted Date: 7 November 2024

doi: 10.20944/preprints202411.0557.v1

Keywords: breast cancer; anthraquinone; Iodine-124; gold nanoparticle

 doi:10.20944/preprints202411.0557.v1

Article

I-124 Labeled Anthraquinone-Derivative-Coating Gold Nanoparticles for Targeted Breast Cancer Diagnosis and Therapy

Jun Young Lee and Jeong Hoon Park *

Cyclotron Application Research Section, Korea Atomic Energy Research Institute, Jeongeup 580-185, Republic of Korea
* Correspondence: parkjh@kaeri.re.kr; Tel.: +82-63-570-3571

Abstract: Background: Rhein, an anthraquinone derivative, and gold nanoparticles have demonstrated significant potential in facilitating the theranostics of breast cancer. Rhein inhibits breast cancer by exhibiting a strong binding affinity to the estrogen receptor. In addition, gold nanoparticles, when used as nanocarriers, may enhance the therapeutic effects against breast cancer. This study outlines the preparation of [^{124}I]rhein-gold for position emission tomography (PET) imaging in a breast cancer mouse model. Method: Gold nanoparticles (30 nm) were prepared using the citrate reduction method. Second, the anthraquinone derivative rhein-cysteine complex was synthesized using the carbodiimide coupling method. Third, the radiosynthesis of [^{124}I]rhein-Cys-gold nanocomposites (RCGs) was performed using the chloramine T method. Specifically, 1 mg of RCGs in dimethylformamide was mixed with Na^{124}I (37 MBq) at pH 12 along with chloramine T (5 mg). The reaction was allowed to proceed for 15 min at room temperature. To remove free ^{124}I, the mixture was purified via centrifugation for 10 min at 10,000 rpm. Results: The radiochemical yield of [^{124}I]RCGs was 65% ± 8.2%, with a radiochemical purity of > 98%. In vivo [^{124}I]RCGs targeted MCF-7 cells in a hormone-dependent manner, with cellular uptake values of 25.4 ± 1.59% at 15 min, 27.1 ± 1.27% at 30 min, 28.6 ± 0.38% at 60 min, and 15.97 ± 0.66% at 120 min. In vivo small-animal PET images of [^{124}I]RCGs showed significant uptake in human breast cancer and MCF-7 tumors. Conclusion: This study demonstrated the synthesis and biological evaluation of [^{124}I]RCGs. [^{124}I]RCGs showed high cellular uptake in a time-dependent manner. PET images of [^{124}I]RCGs confirmed their high affinity for MCF-7 tumors in mice from 1 h to 24 h. These results suggest that [^{124}I]RCGs are promising radiopharmaceuticals, demonstrating potential both as an imaging agent and therapeutic option for estrogen-receptor-targeted breast cancer treatment.

Keywords: breast cancer; anthraquinone; Iodine-124; gold nanoparticle

1. Introduction

In recent years, the incidence of breast cancer patients has increased globally. Approximately one-third of individuals diagnosed with early-stage breast cancer will eventually develop metastatic disease [1]. Consequently, early diagnosis is crucial for preventing the metastasis of cancer to other organs. However, the early detection of breast cancer presents significant challenges owing to the asymptomatic nature of the disease [2,3]. To address this issue, prior research has focused on the identification of overexpressed receptors in breast cancer to aid early diagnosis [4,5]. Rhein, an anthraquinone derivative, has been noted to suppress various human cancer cell types, including those in the breast, colon, and lung [6]. The estrogen receptor (ER) is expressed in approximately 75% of breast cancer patients who are ER-positive and whose tumor growth is driven by endogenous estrogens [7–9]. The level of ER expression is a critical factor influencing the proliferation of breast cancer [10]. Studies have examined the expression of estrogen-α (ERα) in MCF-7 cells, as well as the absence of functional ERα in SK-BR-3 cells [11,12]. Rhein, derived from Rheum palmatum L., Cassia

 doi:10.20944/preprints202411.0557.v1

tora L., and Polygonum multiflorum Thunb, exhibits potent antioxidant and anticancer properties [13]. Consequently, there is a growing need for further research on anthraquinone derivatives that can effectively target breast cancer. Gold nanoparticle (GNP)-based nanocarriers have been used in the treatment of various cancers [Ref]. GNPs smaller than 100 nm are phagocytosed via scavenger receptor-mediated phagocytosis [14,15]. Gold, with its high atomic number (Z = 79), can enhance targeted radiation effects when used with radioisotopes such as Iodine-125 (^{125}I) in biological systems [16,17]. Given these properties, numerous researchers have explored the application of GNPs in cancer treatment using radiation sources [18].

Considering these aspects, this study was aimed at examining the feasibility of establishing a breast cancer treatment using anthraquinone-derivative-coated gold nanocomposites in conjunction with iodine-124 (^{124}I) for positron emission tomography (PET) imaging. The positron-emitting halogen ^{124}I has a long half-life ($t_{1/2}$ = 4.2 d), rendering it suitable for use as a PET imaging agent. The PET imaging capabilities of ^{124}I are particularly beneficial for this study, as it offers specific images with high spatial and contrast resolution [19]. This report presents the evaluation of ^{124}I-labeled anthraquinone-derivative-immobilized GNPs for ERα-targeted PET imaging.

2. Materials and Methods

2.1. Materials and Equipment

Rhein (4,5-dihydroxy-9,10-dioxoanthracene-2-carboxylic acid), sodium citrate dihydrate, N-hydroxysuccinimide (NHS), 1-ethyl-3-(3-dimethylaminopropyl) carbodiimide (EDC), 4-(2-hydroxyethyl)piperazine-1-ethanesulfonic acid (HEPES buffer solution), L-cysteine (Cys), chloramine T (N-chloro-p-toluenesulfonamide sodium salt), bovine serum albumin (BSA), and hydrogen tetrachloroaurate (III) hydrate ($HAuCl_4 \cdot 3H_2O$) were purchased from Sigma-Aldrich. All solvents were used without further purification. ^{124}I was obtained from the Korea Institute of Radiological and Medical Sciences (KIRAMS). All cancer cell lines were acquired from the American Type Culture Collection (ATCC).

Ultraviolet–visible (UV–vis) spectroscopy (Shimadzu UV-1800, Japan) was performed to measure the UV–vis absorbance of Au, Au-Cys, and Au-Cys-Rhein systems. The size and shape of the rhein-immobilized gold nanocomposites were evaluated using transmission electron microscopy (TEM, S-4200, Hitachi, Japan). Hydrodynamic size and ζ-potential measurements were conducted using a Zetasizer (Nano ZS, Malvern Instruments Ltd). Radioactive nanocomposites were characterized using the following equipment: Radiochemical purity was assessed through radio-instant thin layer chromatography (Radio-iTLC, ZR-2000, Bioscan). The activity of the nanocomposite was measured using a dose calibrator (CRC-15R, Capintec). In vitro cellular uptake and biodistribution were determined using a gamma counter (1470 WIZARD2, PerkinElmer).

2.2. Preparation and Characterization of Citrate-Stabilized Gold Nanocomposites

2.2.1. GNP Preparation

GNPs (30 nm) were synthesized using a modified citrate reduction method. Prior to synthesis, all glassware was treated with aqua regia (3:1 HCl/HNO_3) and thoroughly dried. First, 10 mg of $HAuCl_4 \cdot 3H_2O$ was dissolved in 100 mL of distilled water. Next, 0.9 mL of a 3.5 mM sodium citrate dihydrate solution was rapidly added to the mixture. The solution was refluxed at 100 °C for 15 min, during which the color changed from yellow to red. Finally, the solution was allowed to cool to room temperature.

2.2.2. Preparation of Rhein-Cys-GNPs (RCGs)

The rhein-cysteine complex was synthesized using the carbodiimide coupling method. First, 0.04 mmol of rhein was suspended in 700 μL of HEPES buffer solution. Next, 38 mmol of NHS and 31 mmol of EDC were added as coupling agents, and the reaction was allowed to proceed for 24 h at room temperature. The mixture was then centrifuged. Subsequently, 100 μL of a 0.04 mmol L-cysteine solution was slowly added to the activated carboxyl group solution containing rhein. Finally, the

 doi:10.20944/preprints202411.0557.v1

rhein-cysteine complex was introduced into a 30 nm gold colloidal solution, and Rhein-Cys-GNPs were formed through ultrasonic treatment in a bath for 30 min. The resulting gold nanocomposites were washed with distilled water, filtered, and dried at room temperature.

2.3. Radiolabeling of ^{124}I- Rhein and RCGs

2.3.1. ^{124}I-Labeled Anthraquinone Derivative

Before labeling the RCGs with ^{124}I, the labeling efficiency of ^{124}I on rhein was evaluated. First, 2 mg of rhein was dissolved in 200 μL of dimethylformamide (DMF), followed by the addition of Na[^{124}I] (37 MBq). Next, 5 mg of chloramine T was added as an oxidizing agent, and the reaction was allowed to proceed at room temperature for 15 min. After the reaction, the ^{124}I-labeled rhein was purified using a reverse-phase high-performance liquid chromatography (RP-HPLC) system. A mobile phase consisting of 0.25 M ammonium acetate and methanol (MeOH) in a 3:7 ratio was employed, and a C18 reverse-phase chromatography column was used as the stationary phase.

2.3.2. ^{124}I-Labeled RCGs

To prepare [^{124}I]RCGs, 2 mg of RCGs was resuspended in 200 μL of DMF and allowed to react with Na[^{124}I] (37 MBq) and 5 mg of chloramine T as an oxidizing agent. The reaction was allowed to proceed for 15 min at room temperature (27 °C). The radioactivity of free ^{124}I and ^{124}I-labeled RCGs was measured using a radioisotope dose calibrator. To eliminate free ^{124}I, the mixture was purified by centrifugation at 10,000 rpm for 10 min.

2.4. Serum Stability of [^{124}I]RCGs

To assess the biodegradation of [^{124}I]RCGs, their stability in human serum albumin was evaluated at various time points. Specifically, 3.7 MBq of [^{124}I]RCGs was incubated with 1.0 mL of human serum at 37 °C for durations ranging from 0.25 to 24 h. The samples were subsequently analyzed using radio-TLC, with the mobile phase consisting of a 3:1 mixture of chloroform and methanol.

2.5. Partition Coefficient of [^{124}I]RCGs

The 1-octanol/water partition coefficients (log P) of [^{124}I]RCGs were determined using the shake-flask method. A total of 3.7 MBq of [^{124}I]RCGs was added to a conical tube containing 500 μL of phosphate-buffered saline (pH 7.4) and 500 μL of 1-octanol. The mixture was shaken for 5 min and then centrifuged at 10,000 rpm for an additional 5 min. After centrifugation, the radioactivity in 100 μL of each phase was measured using a γ-counter.

2.6. In Vitro Cell Culture and Cellular Uptake of [^{124}I]RCGs

The in vitro binding affinity of [^{124}I]RCGs to breast cancer cells was evaluated using human breast cancer cell lines. Human breast cancer cells (MCF-7 and SK-BR-3) were routinely cultured in 100 mm culture plates (1×10^5 cells/well) at 37 °C with 5% CO_2 in a humidified atmosphere. The cells were grown in the RPMI 1640 medium supplemented with 10% fetal bovine serum and 1% penicillin (10,000 U/mL) and streptomycin (10,000 μg/mL). Cancer cells were detached and dissociated using a 0.05% trypsin/0.02% EDTA solution for cellular uptake studies. Subsequently, the cancer cells were seeded into 24-well culture plates and incubated under standard conditions. [^{124}I]RCGs were added to each well to assess the cellular uptake at various time points (15, 30, 60, and 120 min).

2.7. In Vivo Establishment of MCF-7 Tumor Model and PET Imaging

Before injecting the MCF-7 cells, an estradiol pellet (0.36 mg, 60-d release) was subcutaneously implanted into the dorsal region of each female athymic nude mouse (6 weeks old, weighing 25–30 g). This procedure provided the necessary estrogen supplementation needed for the growth of ER-positive MCF-7 tumors. After implantation, we waited 1 to 2 d for the pellet to begin releasing

 doi:10.20944/preprints202411.0557.v1

estrogen. Then, 100 μL of the prepared cell suspension containing approximately 1 × 10^6 MCF-7 cells was subcutaneously injected into the right thigh of each mouse for PET imaging. [^{124}I]RCGs were injected intravenously at a dose of 3.7 MBq/100 μL per mouse.

3. Results

3.1. Synthesis and Characterization

To achieve a synergistic combination of GNPs, we synthesized ^{124}I-labeled anthraquinone-coated gold nanocomposites. The preparation of 30 nm GNPs was accomplished through nucleation and growth processes. The strong interaction between thiol groups and gold served as the foundation for the fabrication of robust self-assembled monolayers for coating the anthraquinone derivatives. In general, ^{124}I in the -1 oxidation state occurs through its reaction with chloramine T, an electrophilic species in the +1 oxidation state. This reaction results in the substitution of an activated proton from the aromatic ring of tyrosine at the ortho position relative to the phenol group. The synthesis of the nanocomposites is illustrated in Figure 1. Various analytical methods, including UV spectroscopy, high-performance liquid chromatography (HPLC), dose calibrator measurements, zeta potential analysis, and TEM, were used to characterize the GNPs, rhein, RCGs, and [^{124}I]RCGs.

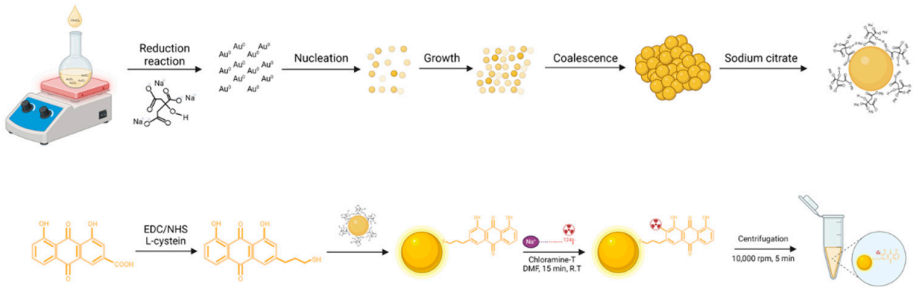

Figure 1. Preparation of nanocomposites for the nucleation and growth of gold nanoparticles coated with anthraquinone derivatives and labeled with ^{124}I (Created in BioRender. Lee, J. (2024) https://BioRender.com/p54g744)

3.1.1. UV–Vis Spectroscopy

The 30 nm gold nanoparticles were characterized using a UV–vis spectrometer over a wavelength range of 300 to 800 nm, with a scan step of 1 nm. The prominent absorption peak observed at 535 nm corresponds to the surface plasmon excitation of 30 nm GNPs [20]. A previous study has shown a similar excitation peak at 525 nm for synthesized GNPs.

 doi:10.20944/preprints202411.0557.v1

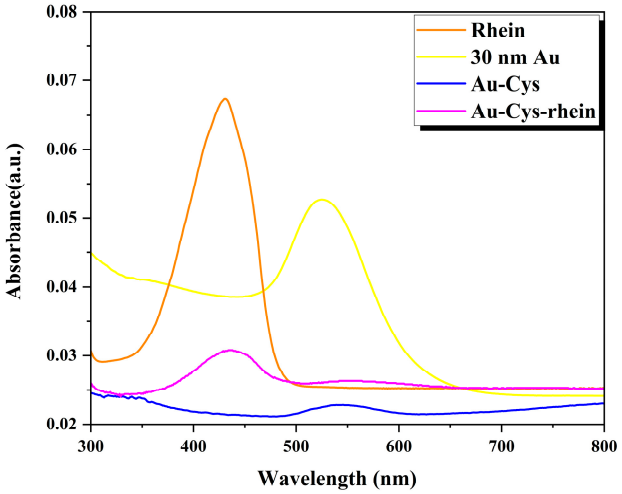

Figure 2. UV-Vis absorption spectra and adsorption shift of gold nanocomposites.

Table 1. Hydrodynamic size and charge of Au, Au-Cys, Au-Cys-rhein.

	Hydrodynamic size (nm)	ζ-potential (mV)
Au	35.0	-42.8
Au-Cys	37.2	-78.7
Au-Cys-rhein	38.4	-48.0

3.1.2. Synthesis of RCGs

The functionalization of GNPs was achieved using L-cysteine as an interface. First, rhein was conjugated to L-cysteine through an EDC/NHS coupling reaction. This conjugate was then attached to citrate-stabilized GNPs. The labeling of ^{124}I onto the RCG nanoparticles was performed using chloramine T as an oxidizing agent.

The thickness of the anthraquinone shell was determined to be between 3 and 4 nm through hydrodynamic size measurements of GNPs, Au-cysteine complexes, and Au-cysteine-rhein complexes. Additionally, the surface charge of these entities was found to be negative.

3.1.3. ^{124}I-Labeled Rhein

To improve the labeling technique of ^{124}I before its application to rhein coated with GNPs, a synthesis study was conducted involving ^{124}I and rhein, employing chloramine T as an oxidizing agent. The radiochemical yield (RCY) of [^{124}I]Rhein was 25–35%, with a radiochemical purity (RCP) exceeding 95%.

Preprints.org (www.preprints.org) | NOT PEER-REVIEWED | Posted: 7 November 2024 doi:10.20944/preprints202411.0557.v1

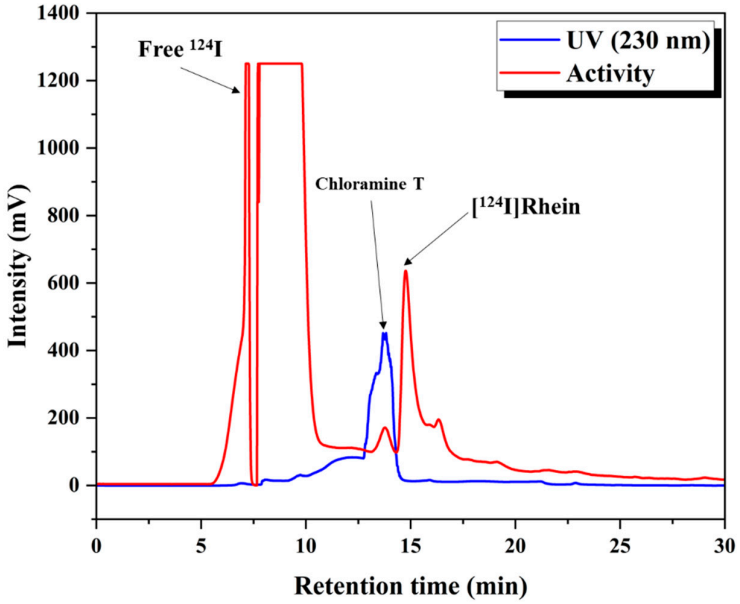

Figure 3. Analysis by HPLC of the iodinated product [^{124}I]Rhein

3.1.4. Synthesis of ^{124}I-Labeled RCGs

The RCY achieved using the established procedure was 65% ± 8.2% (n = 3), with an RCP of 98%, as determined by radio-TLC (mobile phase: 85% MeOH). As in the chloramine T method, the yield was enhanced by increasing the chloramine T, resulting in the successful synthesis of ^{124}I-labeled RCGs.

3.1.5. Partition Coefficient and In Vitro Serum Stability

The partition coefficient (log P) of the ^{124}I-labeled RCGs was assessed in a mixture of 1-octanol and phosphate-buffered saline (pH 7.4). Subsequently, the radioactivity was quantified using a dosimeter, and log P values were calculated. The measured log P value was -0.74 ± 0.06, indicating the hydrophilic nature of the agent. The RCP of the ^{124}I labeled radiolabeled chimeric antibodies (RCGs) exceeded 98% at 15 min and 88% after 24 h. Additionally, the ^{124}I labeled RCGs demonstrated stability exceeding 90% for up to 4 h.

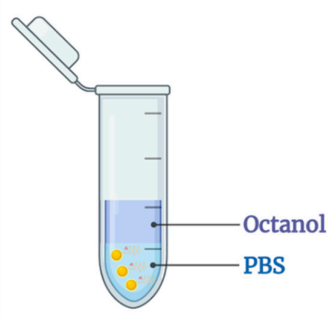

$$LogP = \frac{activity\,(cpm)\,in\ Octanol}{activity\ (cpm)\,in\ PBS}$$

LogP= -0.738 ± 0.098 (Hydrophilic)

Figure 4. Determination of lipophilicity of ^{124}I labeled rhein-cysteine-gold nanocomposites.

 doi:10.20944/preprints202411.0557.v1

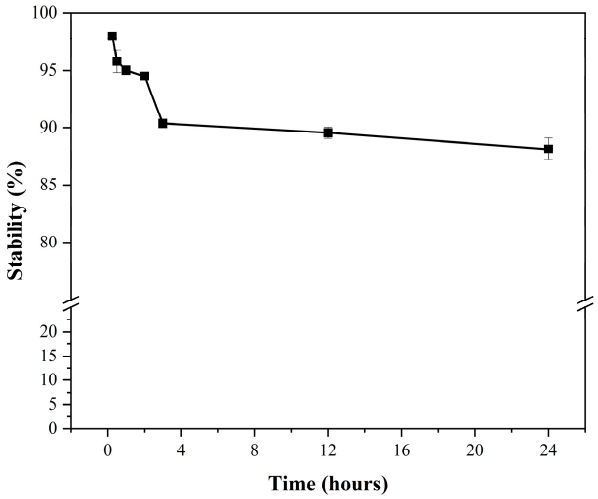

Figure 5. Stability of ^{124}I-labeled RCGs in Human Serum

3.2. In vitro Cellular Uptake

The cellular uptake of human breast cancer cells, specifically the hormone-dependent MCF-7 and hormone-independent SK-BR-3 cell lines, was assessed using [^{124}I]RCGs. The results indicated that [^{124}I]RCGs exhibited a significantly higher uptake in the (ERα)-positive, estrogen-responsive MCF-7 cells after a 60 min incubation period, with uptake percentages of 28.6% for MCF-7 and 24.6% for SK-BR-3. However, the binding affinity of the cells decreased following a 120 min incubation time. These findings indicate that the swift interaction of ERs could serve as a diagnostic tool.

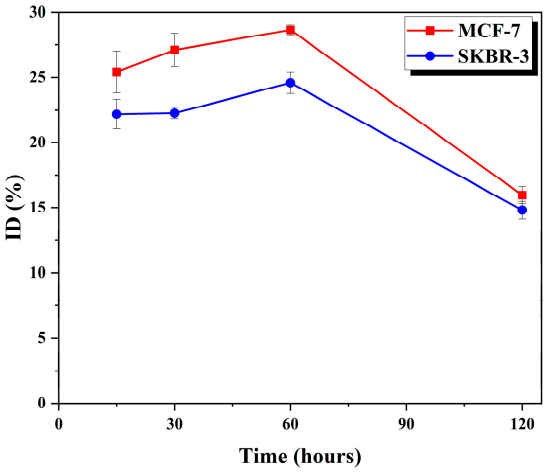

Figure 6. Cellular uptake studies of ^{124}I labeled RCGs. Values are mean ± standard deviation (n=3).

3.3. Small-Animal PET Imaging Experiments

The whole-body distribution of [^{124}I]RCGs in an MCF-7 bearing mouse model is illustrated in Figure 7. The MCF-7 tumors could be distinctly identified, with a high tumor-to-background contrast recorded at various time points (1, 4, 12, and 24 h). The PET images demonstrated significant tumor uptake shortly after intravenous administration. The in vivo specificity of [^{124}I]RCGs was confirmed in an estrogen-α positive tumor, with a high uptake of 8.19 ± 0.99% SUVmax (Figure 7a). Furthermore,

 doi:10.20944/preprints202411.0557.v1

the tumor-to-thyroid ratios were calculated to be 10.53 (Figure 7b). The biodistribution studies conducted on the MCF-7 bearing mouse model for breast cancer suggest that [^{124}I]RCGs may serve as an effective tracer for ERα imaging.

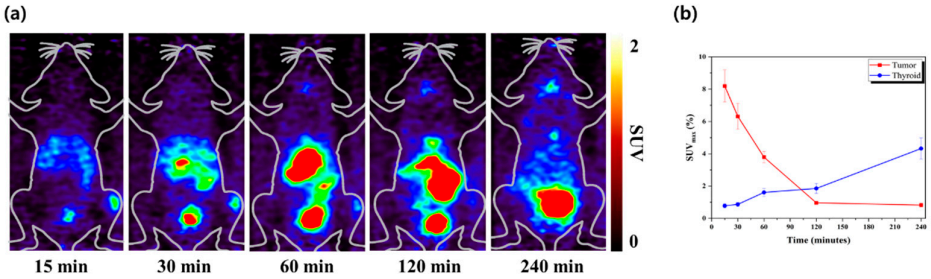

Figure 7. Micro-PET image of ^{124}I-RCGs. (a) Images at different time points post-injection; (b) the metabolic behavior of ^{124}I-RCGs in the tumor and thyroid gland.

4. Discussion

Prior studies have reported that rhein inhibits glucose uptake in tumor cells, leading to membrane-associated functions that induce cell death. To validate the selective accumulation of the estrogen-α receptor, we selected rhein, an anthraquinone derivative, and introduced GNPs labeled with positron emitter ^{124}I for targeted breast cancer imaging. GNPs are being increasingly recognized for their effectiveness in drug delivery owing to their enhanced cellular uptake, biocompatibility, hydrophilicity, non-immunogenicity, and reduced toxicity.

Before labeling the rhein-gold nanocomposites with ^{124}I, the labeling procedure utilizing chloramine oxidizer for [^{124}I]rhein was optimized. After confirming its high reactivity, the synthesized rhein-gold nanocomposite was labeled with ^{124}I in a single-step reaction. To evaluate the accumulation of the rhein-gold nanocomposite in breast cancer cells, the uptake was evaluated in MCF-7 and SKBR-3 breast cancer cell lines, revealing a pronounced tendency for rapid uptake within a 60 min period. Building on these findings, PET imaging studies were performed to confirm the rapid uptake and release of the nanocomposite into the tumor. Overall, we successfully synthesized rhein-coated GNPs labeled with 124I and conducted active targeting assays against the MCF-7 breast cancer cell line that overexpresses estrogen-α receptor, validating their potential as a targeting imaging agent.

5. Conclusions

The study successfully synthesized ^{124}I-labeled rhein-coated gold nanoparticles and demonstrated their potential as targeted PET imaging agents for breast cancer, particularly for estrogen receptor-alpha (ERα) positive tumors. The nanoparticles exhibited significant cellular uptake in ERα-positive MCF-7 cells, confirming their targeting efficiency. Additionally, PET imaging in a mouse model showed high tumor uptake and clear tumor visualization. These findings suggest that ^{124}I-labeled rhein-coated gold nanoparticles could serve as a promising diagnostic tool for early breast cancer detection and imaging.

Author Contributions: Conceptualization; methodology; validation; writing—original draft preparation; writing—review and editing: Jun Young Lee, supervision; project administration; funding acquisition: Jeong Hoon Park. All authors have read and agreed to the published version of the manuscript.

Funding: This study was supported by a National Science and Technology Information Service (NTIS 2710000925 and 2710001996), Republic of Korea.

Institutional Review Board Statement: The study was conducted according to institutional animal care and use committee (IACUC) guidelines provided by Korea Atomic Energy Research Institute (IACUC number: KAERI-IACUC-2024-001).

 doi:10.20944/preprints202411.0557.v1

Informed Consent Statement: Not applicable.

Data Availability Statement: Not applicable.

Acknowledgments: We would like to acknowledge the researchers at the RFT-30 cyclotron facility of the Korea Atomic Energy Research Institute (Jeongeup, Korea) for their contributions to the application of the radioisotope.

Conflicts of Interest: The authors declare no conflict of interest. The funders had no role in the design of the study; in the collection, analyses, or interpretation of data; in the writing of the manuscript, or in the decision to publish the results.

References

1. Maltoni R, Gallerani G, Fici P, Rocca A, and Fabbri F. CTCs in early breast cancer: A path worth taking. Cancer Letters 2016;376:205-10.
2. Pellet AC, Erten MZ, and James TA. Value analysis of postoperative staging imaging for asymptomatic, early-stage breast cancer: implications of clinical variation on utility and cost. The American Journal of Surgery 2015.
3. Minamimoto R, Senda M, Jinnouchi S, Terauchi T, Yoshida T, and Inoue T. Detection of breast cancer in an FDG-PET cancer screening program: results of a nationwide Japanese survey. Clinical breast cancer 2015;15:e139-e46.
4. Lin A and Rugo HS. The role of trastuzumab in early stage breast cancer: current data and treatment recommendations. Current treatment options in oncology 2007;8:47.
5. Iqbal N and Iqbal N. Human epidermal growth factor receptor 2 (HER2) in cancers: overexpression and therapeutic implications. Molecular biology international 2014;2014.
6. Fernand VE, Losso JN, Truax RE, Villar EE, Bwambok DK, Fakayode SO, et al. Rhein inhibits angiogenesis and the viability of hormone-dependent and-independent cancer cells under normoxic or hypoxic conditions in vitro. Chemico-biological interactions 2011;192:220-32.
7. Ronghe A, Chatterjee A, Singh B, Dandawate P, Abdalla F, Bhat NK, et al. 4-(E)-{(p-tolylimino)-methylbenzene-1, 2-diol}, 1 a novel resveratrol analog, differentially regulates estrogen receptors α and β in breast cancer cells. Toxicology and applied pharmacology 2016;301:1-13.
8. Milani A, Geuna E, Mittica G, and Valabrega G. Overcoming endocrine resistance in metastatic breast cancer: current evidence and future directions. World J Clin Oncol 2014;5:990-1001.
9. Singh B, Bhat NK, and Bhat HK. Partial inhibition of estrogen-induced mammary carcinogenesis in rats by tamoxifen: balance between oxidant stress and estrogen responsiveness. PLoS One 2011;6:e25125.
10. Luo A and Zhang X. ERRF is essential for Estrogen-Estrogen Receptor alpha signaling pathway in ER positive breast cancer cells. Biochemical and biophysical research communications 2016;474:400-5.
11. Stoica A, Pentecost E, and Martin MB. Effects of Arsenite on Estrogen Receptor-α Expression and Activity in MCF-7 Breast Cancer Cells 1. Endocrinology 2000;141:3595-602.
12. Lattrich C, Juhasz-Boess I, Ortmann O, and Treeck O. Detection of an elevated HER2 expression in MCF-7 breast cancer cells overexpressing estrogen receptor β1. Oncology reports 2008;19:811-7.
13. Zhou Y-X, Xia W, Yue W, Peng C, Rahman K, and Zhang H. Rhein: a review of pharmacological activities. Evidence-Based Complementary and Alternative Medicine 2015;2015.
14. Ekin A, Karatas OF, Culha M, and Ozen M. Designing a gold nanoparticle-based nanocarrier for microRNA transfection into the prostate and breast cancer cells. The journal of gene medicine 2014;16:331-5.
15. Oh N and Park J-H. Endocytosis and exocytosis of nanoparticles in mammalian cells. Int J Nanomedicine 2014;9:51-63.
16. Daems, N.; Michiels, C.; Lucas, S.; Baatout, S.; Aerts, A. Gold nanoparticles meet medical radionuclides. *Nuclear Medicine and Biology* **2021**, *100*, 61-90.
17. Wang, R.; Liu, H.; Antal, B.; Wolterbeek, H.T.; Denkova, A.G. Ultrasmall Gold Nanoparticles Radiolabeled with Iodine-125 as Potential New Radiopharmaceutical. *ACS Applied Bio Materials* **2024**, *7*, 1240-1249.
18. Chen, Y.; Yang, J.; Fu, S.; Wu, J. Gold nanoparticles as radiosensitizers in cancer radiotherapy. *International Journal of nanomedicine* **2020**, 9407-9430.
19. Braghirolli AMS, Waissmann W, da Silva JB, and dos Santos GR. Production of iodine-124 and its applications in nuclear medicine. Applied Radiation and Isotopes 2014;90:138-48.

 doi:10.20944/preprints202411.0557.v1

20. Ghosh D and Chattopadhyay N. Gold Nanoparticles: Acceptors for Efficient Energy Transfer from the Photoexcited Fluorophores. Optics and Photonics Journal 2013;3:01:9.
21. Castiglione S, Fanciulli M, Bruno T, Evangelista M, Carlo CD, Paggi MG, Chersi A and Floridi A. Rhein inhibits glucose uptake in Ehrlich ascites tumor cells by alteration of membrane-associated functions. Anti-Cancer Drugs 1993;4:407-414.